IEEE P802.15
Wireless Personal Area Networks

Project	IEEE P802.15 Working Group for Wireless Personal Area Networks (WPANs)	
Title	**UWB Channel Model for High Rise Apartments**	
Date Submitted	2 July, 2004	
Source	[Chia-Chin Chong, Youngeil Kim and SeongSoo Lee] [Samsung Advanced Institute of Technology (SAIT)] [i-Networking Lab., P. O. Box 111, Suwon 440-600, Korea.]	Voice: [+82-31-280-6865] Fax: [+82-31-280-9555] E-mail:[chiachin.chong@samsung.com]
Re:	[Response to Call for Contributions on 15.4a Channel Modeling Subgroup.]	
Abstract	[This document describes the UWB channel measurement results in indoor residential environment based in several types of high-rise apartments. It consists of detailed characterization of the frequency-domain parameters, temporal-domain parameters and small-scale amplitude statistics of the UWB channel with bandwidth from 3 to 10 GHz.]	
Purpose		
Notice	This document has been prepared to assist the IEEE P802.15. It is offered as a basis for discussion and is not binding on the contributing individual(s) or organization(s). The material in this document is subject to change in form and content after further study. The contributor(s) reserve(s) the right to add, amend or withdraw material contained herein.	
Release	The contributor acknowledges and accepts that this contribution becomes the property of IEEE and may be made publicly available by P802.15.	

I. INTRODUCTION

The ultra wideband (UWB) indoor propagation channel measurements conducted in various types of high-rise apartments based in several cities in Korea is presented. A vector network analyzer was used to measure the channel transfer functions in the frequency band of 3-10 GHz. The corresponding channel impulse responses were calculated by taking inverse Fourier transforms of the recorded channel transfer functions. Measurements were made in 8-10 distinct receiver (RX) local points throughout the apartment ranging from 1-20 m apart from the fixed transmitter location. At each RX local point; the RX was moved 25 times over a square grid of 5x5 spatial points spaced 15 cm apart. This measurement procedure allows us to characterize both the small-scale and the large-scale statistics of the channel. Various communication links were considered including both line-of-sight (LOS) and non-LOS (NLOS) scenarios. Both data analysis technique and measurement results are presented in the form of path loss and shadowing, temporal domain parameters and small-scale amplitude statistics.

II. MEASUREMENT SETUP AND PROCEDURE

A. Measurement Setup

Measurements were conducted in the frequency-domain in which the channel transfer function (CTF) were measured and stored. The measurement system consists of a vector network analyzer (VNA), a 30 dB gain wideband power amplifier, a 32 dB gain low noise amplifier, an attenuator and a pair of vertically polarized wideband planar dipole antennas [1]. The VNA was remotely controlled by LabVIEW software so that data collection could be done automatically. The measured data from the VNA was then stored on a laptop hard drive via a GPIB interface. Fig. 1 illustrates an overview of the measurement setup. The antenna effects were removed from the channel measurements by calibrating the measurement equipment in an anechoic chamber with respect to a 1 m reference distance. The calibration data was also saved for data analysis and post-processing. During the measurements, the VNA was set to transmit 1601 continuous waves tones uniformly distributed over the 3-10 GHz frequency range (i.e. with center frequency of 6.5 GHz), which results frequency step of 4.375 MHz. This frequency resolution gives maximum excess delay of about 229.6 ns and maximum distance range of approximately 68.6 m. The 7 GHz bandwidth gives a temporal resolution of 142.9 ps. By setting the IF bandwidth of the VNA to 3 kHz, the sweeping time is automatically adjusted to sweep the 7 GHz bandwidth in 800 ms. Thus, the maximum measurable Doppler spread would be 1.25 Hz (i.e. 1/800 ms). The VNA measures the S-parameter, S_{21}, of the UWB channel which is essentially corresponds to the CTF. In order to get reliable channel models, the sweeping time should not exceed the channel coherence time.

B. Measurement Procedure and Environments

Field measurements have been conducted in various types of high-rise apartments based in several cities in Korea. These apartments have different sizes, layouts and structures consist of 3-

5 bedrooms. Both empty and furnished apartments have been investigated. In each apartment, the transmitter (TX) was placed at a fixed position (i.e. in the center of the living room), while the receiver (RX) was moved throughout the apartment around 8-10 different positions with TX-RX separation ranging from 1-20 m. We refer this different RX positions as *local points* [2] . Both line-of-sight (LOS) and non-LOS (NLOS) scenarios were considered which include "within-room" and "room-to-room" propagation conditions where all doors and windows were closed during the measurements. Two levels of measurements were performed in order to characterize both the small-scale and large-scale fading parameters of the channel. The random placements of RX throughout the apartment characterize the large-scale behavior of the channel. In order to characterize the small-scale statistics of the channel, the RX was moved 25 times around each local point. These 25 spatial measurements were arranged over a 5×5 square grid with
15 cm spacing between adjacent points. Each point on the grid is referred as a *spatial point* [2]. Fig. 2 and Fig. 3 illustrate the sketched plan of the 3-bedrooms and 4-bedrooms apartments, respectively, and Fig. 4 shows some photos taken during the measurement campaign in the 4-bedrooms apartment. The height of both TX and RX antennas was fixed with the same height i.e. at 1.25 m from the floor and from the ceiling so that they are in the same horizontal plane. During the measurements, both TX and RX antennas and the channel were kept stationary by ensuring there was no movement in the physical surrounding environment. However, in order confirm the time-invariant nature of the channel and for statistical analysis reliability, at each spatial point, 30 time-snapshots of the complex CTFs were recorded. The measured CTFs showed no perceptible differences as illustrated in Fig. 5 for the normalized 3-D CTF at a spatial point over the 30 time-snapshots. Fig. 6 shows the corresponding time-average normalized 2-D CTF at a spatial point (i.e. average over the 30 time-snapshots). Thus, we can conclude that the channel was static over the measured time frames. 750 CTFs were collected at each local point and more than 6,000 complex channel responses per apartment were stored in our database for further analysis.

III. DATA ANALYSIS AND POST-PROCESSING

Before any statistical channel modeling work can be carried out, the first step is to perform appropriate data analysis technique in order to extract the channel parameters of interest from the measurement data. The data analysis procedures can be summarized as follows:

1. Since the VNA measured the transfer function of the "radio channel" (i.e. including the effect of amplifiers, cables and antennas), in order to remove these hardware effects, all measurement data are calibrated with the calibration data measured in anechoic chamber to remove the effect of the measurement system in order to ensure only the "propagation channel" transfer function will be used for further analysis.
2. By assuming that the channel is static, averaging is carried out over the temporal domain for each block of 30 time-snapshots of CTFs measured at each spatial point. This assumption is justified since no movement was allowed during the measurements.
3. Frequency domain windowing was applied prior to the transformation of the frequency domain data to the time domain data in order to reduce the leakage problem at the expense of

reducing the temporal resolution. The Hamming window is chosen since it has side lobe suppression about 41 dB [3].

4. The windowed CTFs were transformed into the channel impulse responses (CIRs) through inverse Fourier transform (IFT). Here, the real passband IFT processing technique was used instead of the complex baseband IFT technique due to several advantages the former technique offers such as an increase in the temporal resolution by a factor of more than two. Thus, this can overcome the resolution reduction due to the windowing process. A detail comparison between these two techniques is reported in [4].
5. A cutoff threshold of 30 dB below the strongest path was applied to the CIRs to ensure that only the effective paths are used for the channel modeling.
6. The CIRs are then normalized such that the total power in each power delay profile (PDP) is equal to one.
7. The initial delay for each of the transmission links was extracted from the PDP. This value was removed from the results so that all PDPs can be aligned with first path arrives at 0 ns.

IV. PATH LOSS AND SHADOWING

A. Distance Dependence

The path loss in dB as a function distance is given by

$$PL(d) = PL_0 + 10n\log_{10}\left(\frac{d}{d_0}\right) + S; \quad d \geq d_0 \tag{1}$$

where d_0 is the reference distance i.e. $d_0 = 1m$ and PL_0 is the free-space path loss in the far-field of the antennas at a reference distance d_0. PL_0 is the interception point and usually is calculated based on the mid-band frequency. n is the path loss exponent and S is the shadowing fading parameter that varies randomly from one location to another location within any home. It is a zero-mean Gaussian distributed random variables (in dB) with standard deviation σ_S which is also in dB. Fig. 7 and Fig. 8 show the path loss as a function of distance under the LOS and NLOS scenarios in 3-bedroom and 4-bedroom apartments, respectively. Table 1 lists the path loss and shadowing parameters extracted from the measurement data.

B. Frequency Dependence

The frequency dependency of the path loss can be modeled by [5] and [6]

$$\log_{10}(PL(f)) = \alpha\exp(-\delta f) \tag{2}$$

where α is the distance dependent signal attenuation and δ is the *frequency decaying factor* in dB/Oct in which δ is calculated using the least-square curve fitting of (2) on the measured data.

It statistics is characterize by its mean, μ_δ and standard deviation, σ_δ . Table 2 lists the frequency decaying factor parameters extracted from the measurement data.

V. TEMPORAL DOMAIN PARAMETERS

A. Mean Excess Delay and RMS Delay Spread

The *mean excess delay*, τ_m is defined as the first moment of the power delay profile (PDP) and is defined as [7]

$$\tau_m = \frac{\sum_k a_k^2 \tau_k}{\sum_k a_k^2} = \frac{\sum_k P(\tau_k)\tau_k}{\sum_k P(\tau_k)} \tag{3}$$

where a_k , τ_k and $P(\tau_k)$ are the gain coefficient, delay and PDP of the k^{th} multipath component (MPC), respectively. The *rms delay spread*, τ_{rms} is the square root of the second central moment of the PDP and is defined to be [7]

$$\tau_{rms} = \sqrt{\tau_m^2 - (\tau_m)^2} \tag{4}$$

where

$$\tau_m^2 = \frac{\sum_k a_k^2 \tau_k^2}{\sum_k a_k^2} = \frac{\sum_k P(\tau_k)\tau_k^2}{\sum_k P(\tau_k)}. \tag{5}$$

B. Number of Dominant MPCs

To find the number of dominant MPCs, NP , the delay axis is discretized into a number of bins. The selection of the bin size is determined by the measurement resolution. Here, the bin size is set to 100 ps. $NP10dB$, $NP20dB$ and $NP30dB$ is defined as the number of MPCs that arrive within 10 dB, 20 dB and 20 dB of the strongest path for each of the PDP. Fig. 9 and Fig. 10 show the distribution of $NP10dB$, $NP20dB$ and $NP30dB$ under the LOS and NLOS scenarios in 3-bedroom and 4-bedroom apartments, respectively.

Table 3 lists the temporal domain parameters extracted from the measurement data. These parameters were obtained after taking the frequency domain Hamming windowing, the passband IFFT and the temporal domain binning with bin size 100 ps [8].

VI. SMALL-SCALE AMPLITUDE FADING STATISTICS

The empirical distribution of the small-scale amplitude fading is compared with the following four commonly used theoretical distributions:

1. Lognormal
2. Nakagami
3. Rayleigh
4. Weibull

The goodness-of-fit of the small-scale signal amplitudes is evaluated using Kolmogorov-Smirnov (K-S) hypothesis test with 5% significance level to test which of the four distributions best fit the data. Fig. 11 and Fig. 12 show the small-scale amplitude probability density distribution (PDF) at a fixed excess delays (i.e. 50 ns) when measurement data from only one RX location is considered (i.e. consisting of 25 spatial points) for the LOS and NLOS scenarios in 3-bedroom and 4-bedroom apartments, respectively. While Fig. 13 and Fig. 14 show the small-scale amplitude cumulative distribution function (CDF) at different excess delays (i.e. 5 ns, 50 ns and 100 ns) for the LOS and NLOS scenarios in 3-bedroom and 4-bedroom apartments, respectively. Results demonstrate that either lognormal, Nakagami or Weibull distributions can fit the small-scale amplitude fading statistics of the measurement data reasonably well. Table 4 lists the pass rate of the K-S test for the four different theoretical distributions under LOS and NLOS scenarios in 3-bedroom and 4-bedroom apartments.

Parameters of these distributions (i.e. standard deviation of the lognormal PDF, σ_L, *m*-parameter of the Nakagami PDF, m_N, and shape parameter of the Weibull PDF, b_W) remain almost constant across the excess delay. Their statistics are characterized by their corresponding mean and standard deviation, respectively. Table 5 lists the mean and standard deviation of these parameters under LOS and NLOS scenarios in 3-bedroom and 4-bedroom apartments.

REFERENCES

[1] D. -H. Kwon and Y. Kim, "CPW-fed planar ultra-wideband antenna with hexagonal radiating elements." *IEEE Intl. Symp. on Antennas and Propagation 2004*, Monterey, CA, USA, Jun. 2004.

[2] S. S. Ghassemzadeh, L. J. Greenstein, A. Kavcic, T. Sveinsson and V. Tarokh, "UWB indoor path loss model for residential and commercial buildings," in *Proc. IEEE Veh. Technol. Conf. (VTC 2003-Fall)*, Orlando, FL, USA, Sep. 2003, pp. 629-633.

[3] A. V. Oppenheim and R. W. Schafer, *Discrete-Time Signal Processing*, Prentice Hall, Upper Saddle River, NJ, USA, 2nd edition, 1999.

[4] B. Denis and J. Keignart, "Post-processing framework for enhanced UWB channel modeling from band-limited measuremnts," in *Proc. IEEE Conf. UWB Systems and Technologies (UWBST03)*, Reston, VA, USA, Nov 2003, pp. 260-264.

[5] A. Alvarez, G. Valera, M. Lobeira, R. P. Torres and J. L. Garcia, "New channel impulse response model for UWB indoor system simulations," in *Proc. IEEE Veh. Technol. Conf. (VTC 2003-Spring)*, Jeju, Korea, May 2003, pp. 1-5.

[6] A. F. Molisch, "Status of models for UWB propagation channels," IEEE P802.15-04/195r0, Mar. 2004.
[7] T. S. Rappaport, *Wireless Communications: Principles and Practice*, Prentice Hall PTR, Upper Saddle River, NJ, USA, 2nd edition, 2002.
[8] Chia-Chin Chong, Y, Kim and S. S. Lee, "UWB indoor propagation channel measurements and data analysis in various types of high-rise apartments," *IEEE Veh. Technol. Conf. (VTC 2004-Fall)*, Los Angeles, CA, USA, Sep. 2004, to be presented.
[9] A. A. M. Saleh and R. A. Valenzuela, "A statistical model for indoor multipath propagation," *IEEE J. Select. Areas Commun.*, vol. 5, no. 2, pp. 128-137, Feb. 1987.
[10] A. F. Molisch, U. G. Schuster and Chia-Chin Chong, "Measurement Procedure and Methods on Channel Parameter Extraction," IEEE P802.15-04/283r0, May 2004.

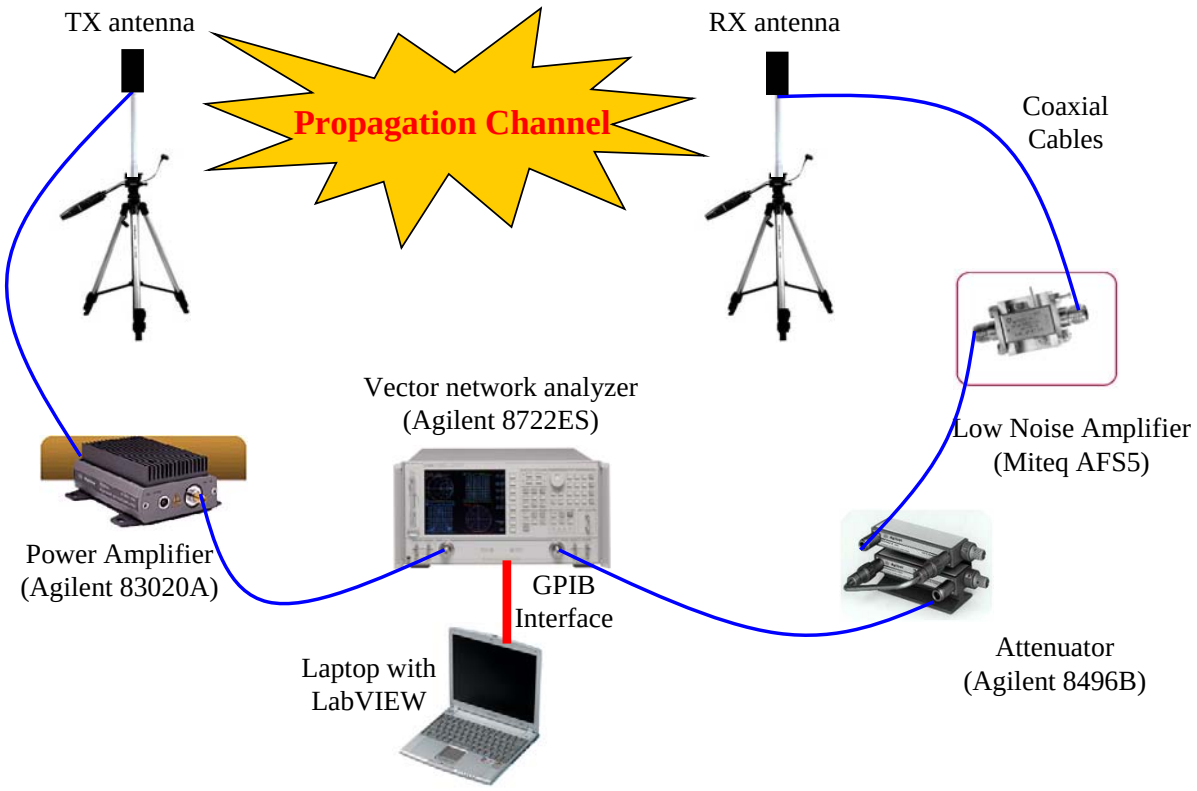

Fig. 1: Overview of the measurement setup.

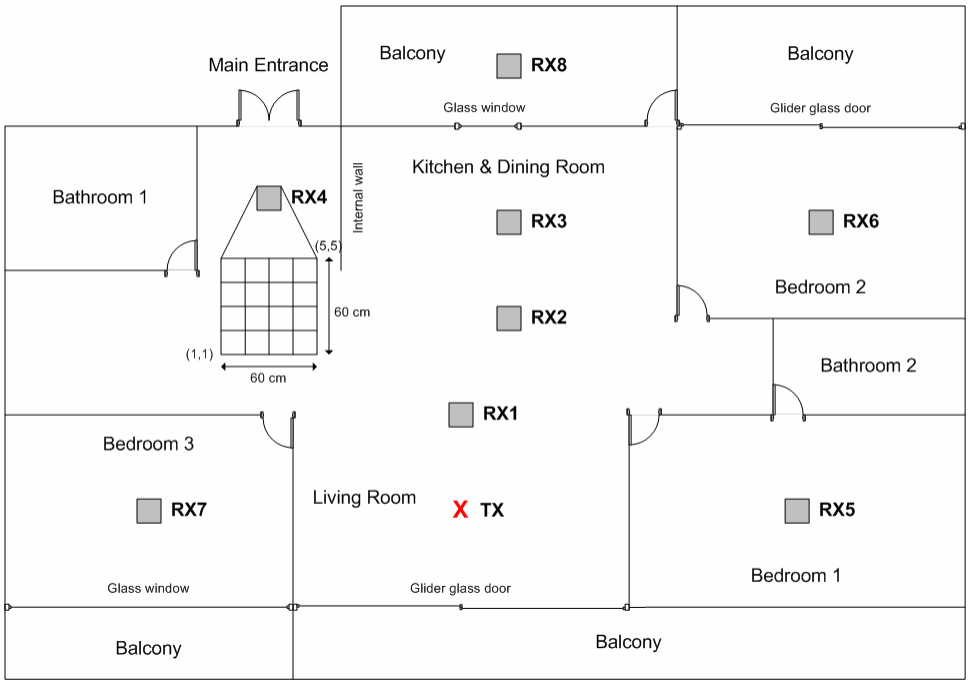

Fig. 2: Sketched plan of the 3-bedrooms apartment.

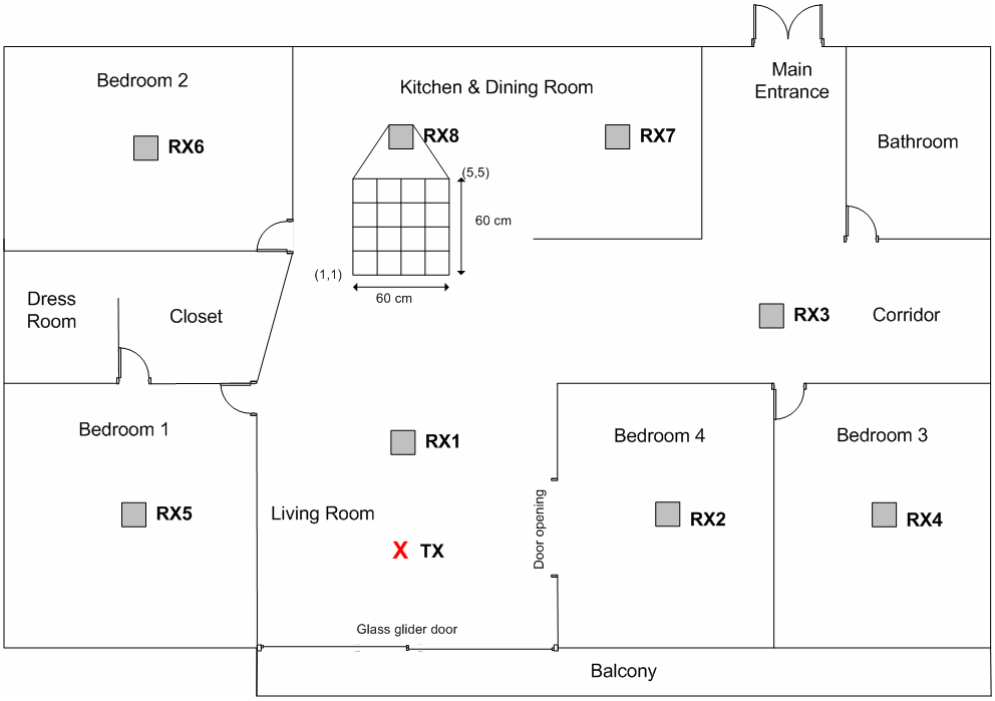

Fig. 3: Sketched plan of the 4-bedrooms apartment.

Fig. 4: Photos taken during the measurement campaign in the 4-bedrooms apartment.

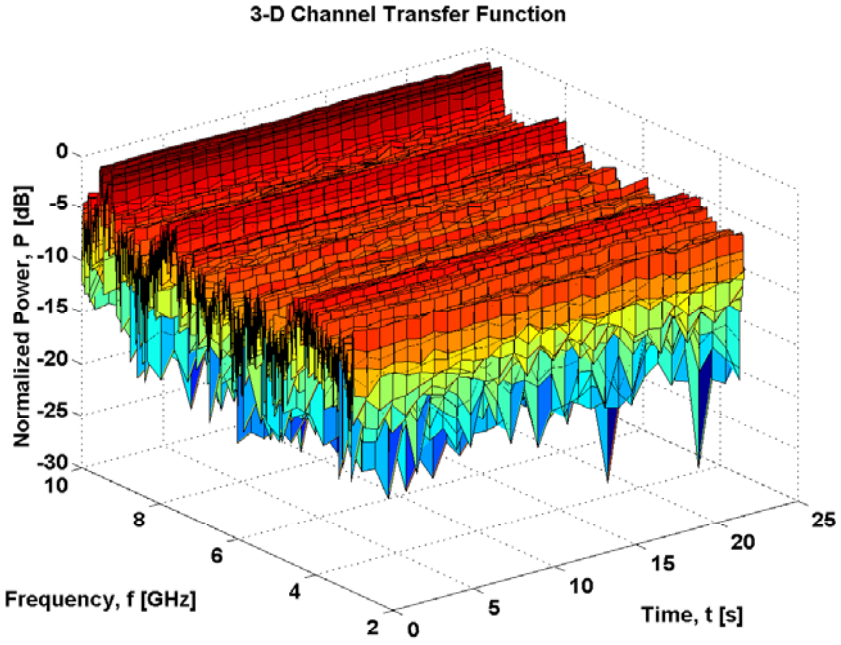

Fig. 5: Normalized 3-D channel transfer function at a spatial point over the 30 time-snapshots.

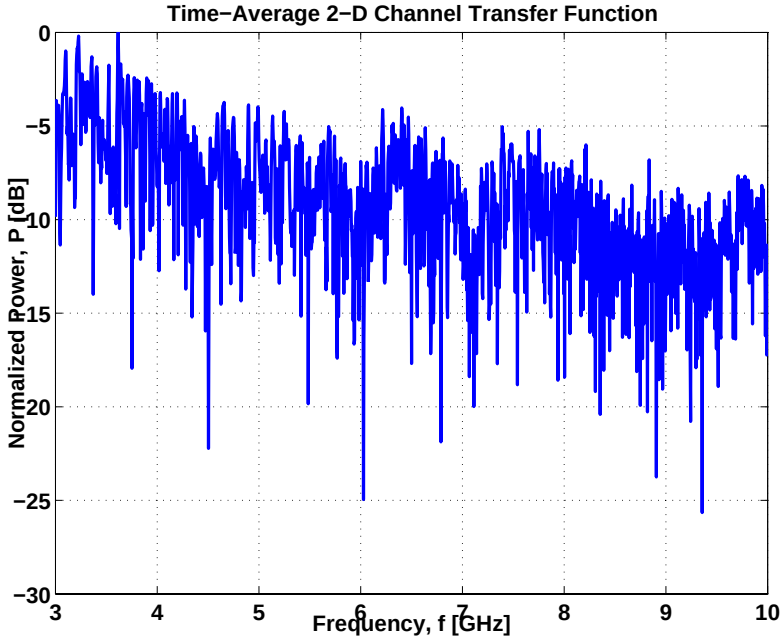

Fig. 6: Time-average normalized 2-D channel transfer function at a spatial point.

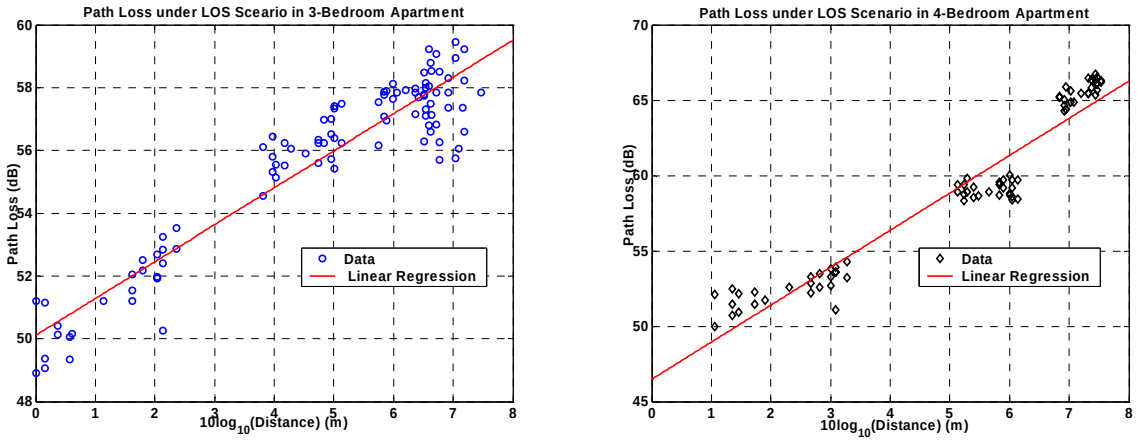

Fig. 7: Path loss as a function of distance under LOS scenario in (a) 3-bedroom apartment and (b) 4-bedroom apartment, respectively.

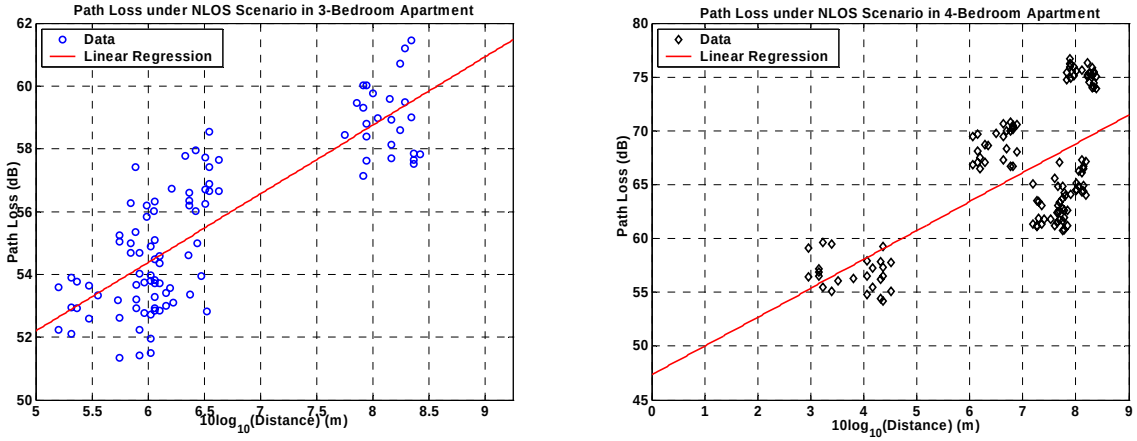

Fig. 8: Path loss as a function of distance under NLOS scenario in (a) 3-bedroom apartment and (b) 4-bedroom apartment, respectively.

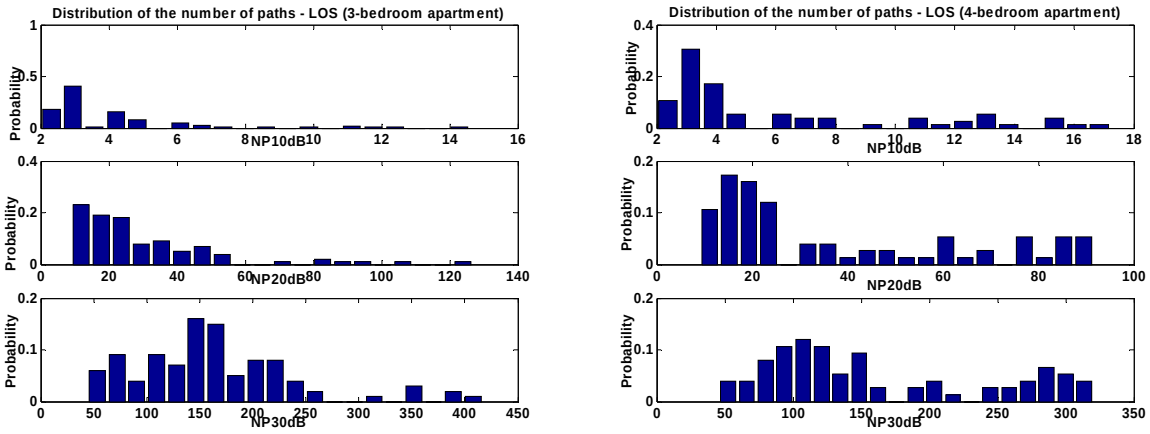

Fig. 9: Distribution of the number of dominant MPCs (i.e. $NP10dB$, $NP20dB$ and $NP30dB$) under LOS scenario in (a) 3-bedroom apartment and (b) 4-bedroom apartment, respectively.

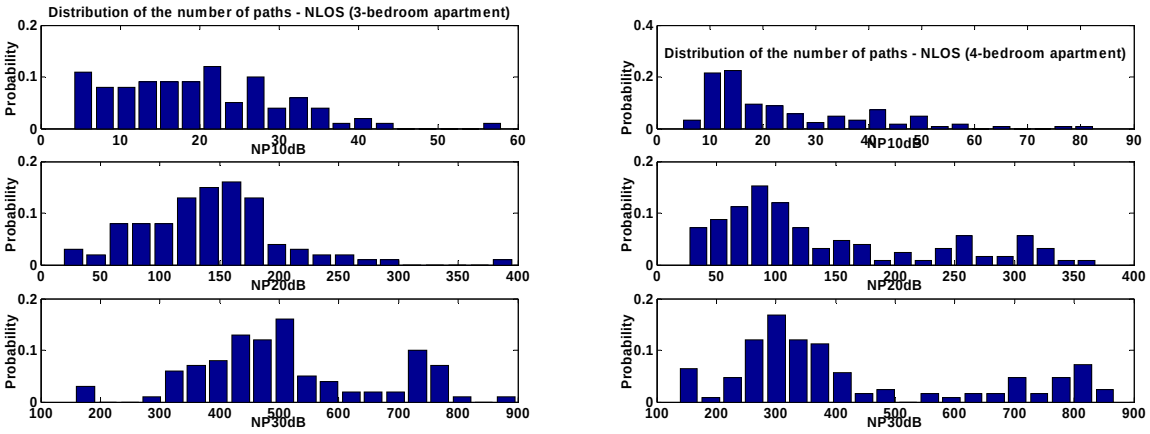

Fig. 10: Distribution of the number of dominant MPCs (i.e. $NP10dB$, $NP20dB$ and $NP30dB$) under NLOS scenario in (a) 3-bedroom apartment and (b) 4-bedroom apartment, respectively.

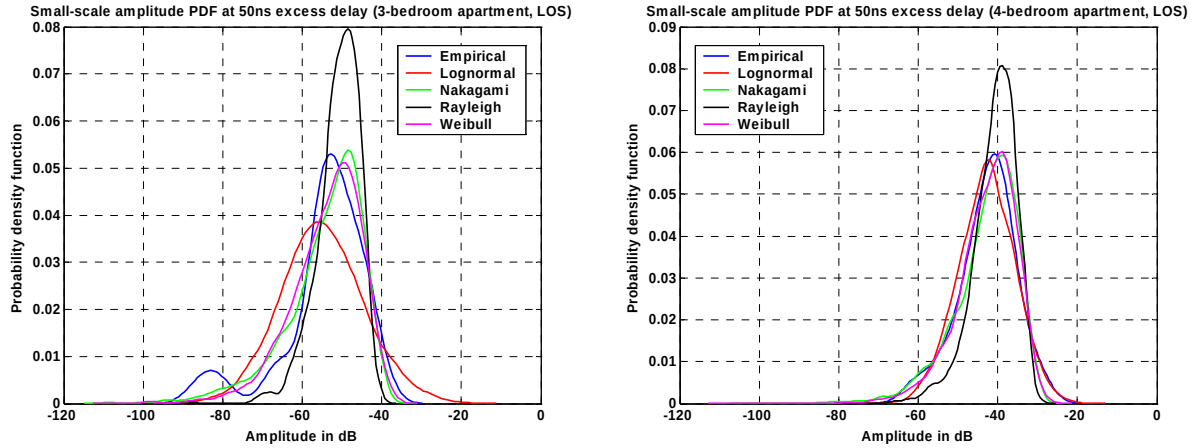

Fig. 11: Small-scale amplitude PDF at 50 ns excess delays under LOS scenario in (a) 3-bedroom apartment and (b) 4-bedroom apartment, respectively.

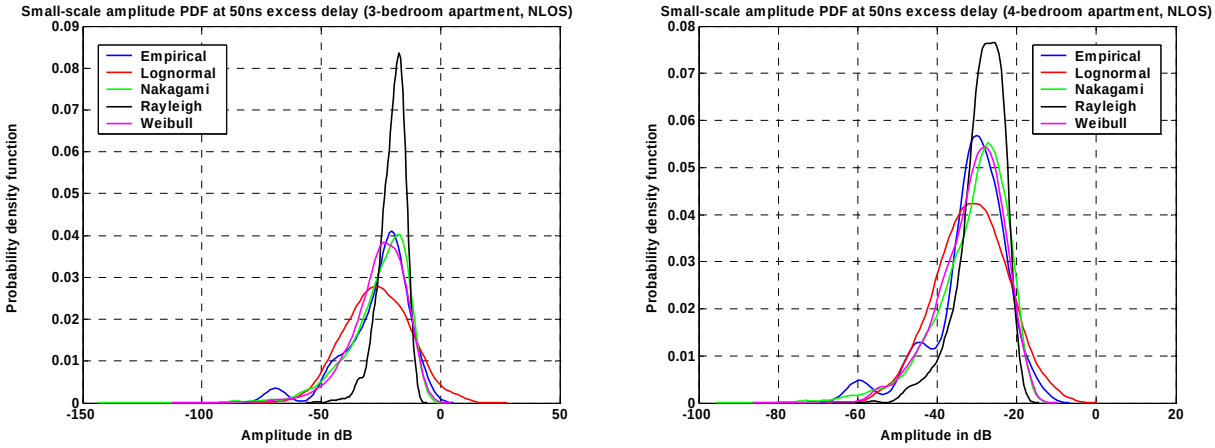

Fig. 12: Small-scale amplitude PDF at 50 ns excess delays under NLOS scenario in (a) 3-bedroom apartment and (b) 4-bedroom apartment, respectively.

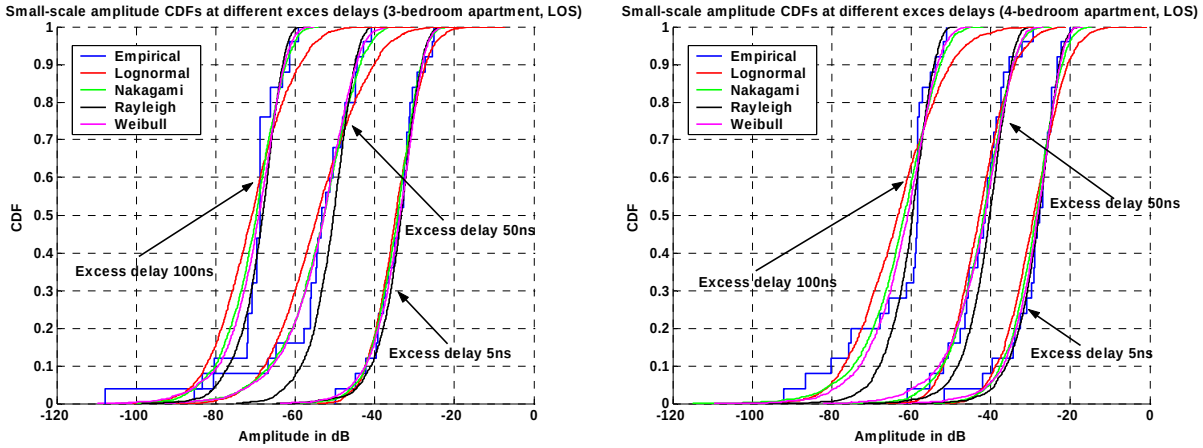

Fig. 13: Small-scale amplitude CDF at different excess delays under LOS scenario in (a) 3-bedroom apartment and (b) 4-bedroom apartment, respectively.

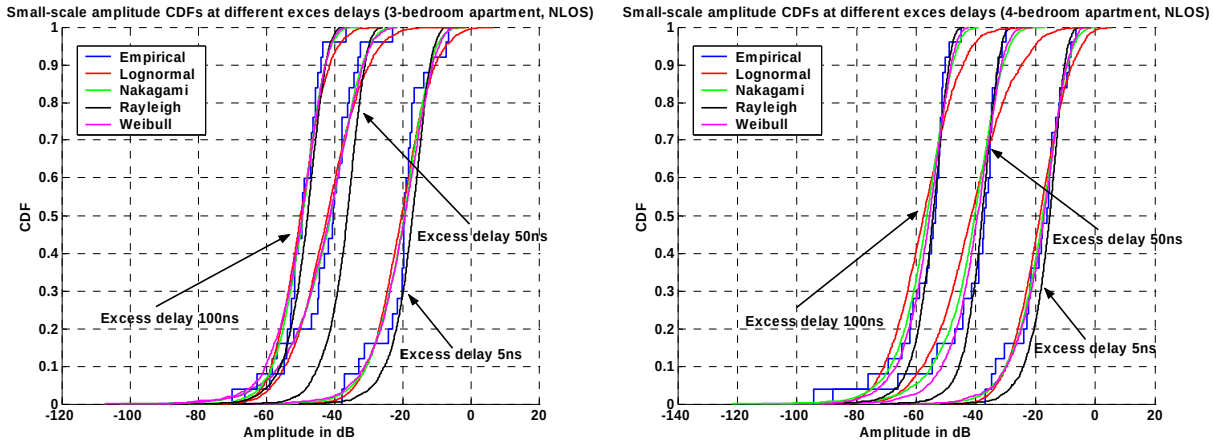

Fig. 14: Small-scale amplitude CDF at different excess delays under NLOS scenario in (a) 3-bedroom apartment and (b) 4-bedroom apartment, respectively.

Scenario	3-Bedroom Apartment			4-Bedroom Apartment		
	n	PL_0	σ_S	n	PL_0	σ_S
LOS	1.18	50.1	0.93	2.48	49.7	1.50
NLOS	2.18	52.2	1.43	2.69	52.7	4.69

Table 1: Path loss and shadowing parameters.

Location	3-Bedroom Apartment		4-Bedroom Apartment	
	μ_δ [dB/Oct]	σ_δ [dB/Oct]	μ_δ [dB/Oct]	σ_δ [dB/Oct]
LOS	0.5903	0.0993	0.8434	0.1324
NLOS	0.7431	0.2145	1.1695	0.3842

Table 2: Frequency decaying factor parameters.

Location	τ_m		τ_{rms}		$NP10dB$		$NP20dB$		$NP30dB$	
	μ_{τ_m}	σ_{τ_m}	$\mu_{\tau_{rms}}$	$\sigma_{\tau_{rms}}$	μ_{NP10dB}	σ_{NP10dB}	μ_{NP20dB}	σ_{NP20dB}	μ_{NP30dB}	σ_{NP30dB}
LOS (3-Bedroom Apartment)	5.88	1.25	14.00	1.53	4.04	1.53	29.91	11.15	145.38	38.89
NLOS (3-Bedroom Apartment)	36.09	15.48	38.61	8.03	19.58	7.64	141.63	42.23	512.57	76.28
LOS (4-Bedroom Apartment)	5.01	0.64	12.48	1.87	5.97	1.96	37.21	9.20	161.02	31.59
NLOS (4-Bedroom Apartment)	24.95	8.47	26.51	5.22	23.51	10.75	139.95	50.14	424.78	93.77

Table 3: Temporal domain parameters.

Location	K-S Test Pass Rate (%)			
	Lognormal	Nakagami	Rayleigh	Weibull
LOS (3-Bedroom Apartment)	90.42	91.42	58.56	92.99
NLOS (3-Bedroom Apartment)	89.81	88.68	49.72	88.81
LOS (4-Bedroom Apartment)	80.49	81.83	50.78	81.64
NLOS (4-Bedroom Apartment)	86.16	83.60	44.51	83.76

Table 4: Small-scale amplitude statistics K-S hypothesis test past rate for different theoretical distributions.

Location	σ-Lognormal Parameter		*m*-Nakagami Parameter		*b*-Weibull Parameter	
	μ_{σ_L}	σ_{σ_L}	μ_{m_N}	σ_{m_N}	μ_{b_W}	σ_{b_W}
LOS (3-Bedroom Apartment)	0.9876	0.2558	0.5485	0.2173	1.3319	0.2620
NLOS (3-Bedroom Apartment)	1.0218	0.3607	0.5528	0.1671	1.3283	0.3114
LOS (4-Bedroom Apartment)	0.9910	0.2701	0.5232	0.1557	1.3045	0.2649
NLOS (4-Bedroom Apartment)	1.0082	0.2647	0.9048	0.3300	1.6082	0.2439

Table 5: Mean and standard deviation of the lognormal, Nakagami and Weibull distributions parameters under LOS and NLOS scenarios in 3-bedroom and 4-bedroom apartments.